Desalination and Water Treatment
www.deswater.com
doi: 10.5004/dwt.2023.29786

303 (2023) 245–255
August

Efficient application of Jordanian glass sand for the adsorptive removal of methylene blue from aqueous media

Rasheed M.A.Q. Jamhour[a,*], Ashraf Al-Msiedeen[a], Monther Al-Bashabsheh[a], Husam Hani[a], Mohannad R. Jamhour[b]

[a]*Department of Chemistry and Chemical Technology, Tafila Technical University, P.O. Box: 179, Tafila-66110, Jordan, Tel.: +962 799410621; email: rasheedjamhour@gmail.com (R.M.A.Q. Jamhour), Tel.: +962 792269139; emails: ashraf_ttu@yahoo.com (A. Al-Msiedeen), motheryaser@gmail.com (M. Al-Bashabsheh), hussamhani93@gmail.com (H. Hani)*
[b]*Department of Clinical Medical Sciences (CMS), Faculty of Medicine, Yarmouk University, P.O. Box: 566, Irbid-21163, Jordan, Tel.: +962 799457656; email: mohannadrasheed955@gmail.com (M.R. Jamhour)*

Received 8 May 2023; Accepted 12 July 2023

ABSTRACT

Silicates are the pure source of silica sand or glass sand found in vast amounts in south Jordan. It is worth studying the ability of silica glass sand (SGS) powder prepared from natural silica sand to act as an adsorbent to remove methylene blue (MB) dye from polluted water. The SGS material was systematically analyzed by various spectroscopic techniques. The various experimental factors such as dosage, MB concentration, pH, contact time, and temperature, were evaluated. Adsorption isotherms and kinetics data were studied by the pseudo-first-order, pseudo-second-order, and intraparticle diffusion models. The thermodynamic parameters, $\Delta G°$, $\Delta H°$, and $\Delta S°$ were computed and found to be, 0.438 kJ/mol, –3.20 kJ/mol, and –8.613 J/mol·K, respectively. The results indicated that the maximum removal of MB dye was found at low pH values. The collected isotherm data were best fitted by the Langmuir isotherm, and the maximum adsorption capacity of dye onto SGS was 3.28 mg/g. The thermodynamic results demonstrated that the adsorption of the MB occurs spontaneously as an exothermic process. The results confirmed the effectiveness of the prepared low-cost silica sand (SGS) as an adsorbent with excellent recyclability for the remediation of water contaminated by MB dye generated from industry.

Keywords: Adsorption; Kinetics; Dye; Silica sand; Methylene blue

1. Introduction

The utilization of natural low-cost adsorbents for the efficient removal of contaminants in the water is known to be an interesting area of research. The unique properties of such materials for the removal of both organic and inorganic pollutants with high efficiency provide an increasing demand for extensive studies by researchers [1–5]. Various industries, including textile, leather tanning, paper and pulp, printing, dying, food additives, paint, pigments, and pharmaceutical industries, consume a large volume of water during the dyeing process of their products and generate a large amount of colored wastewater, resulting in the continuous discharge of dye contaminants into bodies of water, causing water pollution [6–10]. Synthetic dyes, which are nondegradable pollute the water resources, even at low concentrations, and affect human health [11]. Among the most used industrial dyes, methylene blue (MB) is a basic dyestuff widely used in industry for various purposes. Moreover, the presence of trace amounts of such micro-pollutants discharged from various industrial wastewater is extremely noticeable and has become a

* Corresponding author.

global phenomenon [12]. MB can be found in water because of industrial discharge, agricultural runoff, or accidental spills. It can be introduced through various sources and can have toxic effects on aquatic organisms, especially at high concentrations. It can also disrupt the photosynthetic process in algae and decrease dissolved oxygen levels, which can lead to fish kills [13]. In addition, MB can be harmful to human health if ingested or absorbed through the skin. Some azo dyes have been found to be potentially carcinogenic, meaning they could cause cancer. Azo dyes are synthetic dyes containing one or more azo (–N=N–) groups. These dyes are widely used in various industries, including textile, printing, and food. While not all azo dyes are toxic, some studies have shown that certain azo dyes can have adverse effects on human health and the environment such as MB dye [14]. Also, MB is a non-biodegradable dye in the aquatic system and its usage needs significant attention therefore, it is important to monitor the levels of MB in water and take steps to remove it from wastewater before discharging into an aquatic environment. It is noteworthy that the chemical composition and shape of silica particles can be also factors contributing to toxicity. In this context, silica glass sand (SGS) with adsorbed MB may enhance and lead to irreversible cell damage through oxidative stress and organelle injury with their cellular penetration and translocation ability. Other than penetration, electrostatic charges, van der Waals forces, interfacial tension effects, and steric interaction of SGS bind with cellular components and cause cell death [15]. It can also create reactive oxygen species and cause cellular damage via lipid peroxidation, protein alteration, DNA disruption, signaling function interference, and gene transcription modulation [16,17]. Many treatment methods and techniques have been developed that can be used to remove MB from water, such as activated carbon adsorption, advanced oxidation, and decolorization [18], photocatalytic degradation [19], ultrafiltration [20], and electrochemical treatment [21]. Among these various physico-chemical processes, adsorption is a technique of choice due to its feasibility, low cost, and straightforward design. In the past decade, adsorption has been established as one of the most reliable techniques for water treatment [22–24]. The authors have successfully utilized several novel adsorbents for the removal of various pollutants including metal ions and dyes. It is to be mentioned that nanoparticles at various categories of natural and synthetic adsorbents were also used as low-cost adsorbents for the removal of organic dyes from aqueous media, such as layered double hydroxides clay (LDH), prepared by our group [25] or hydrotalcite [26], zeolite [27], activated carbon [28], mesoporous materials [29], chitosan [30], silica [31], and activated montmorillonite nanocomposite [32]. Aluminosilicates are used as precursors in several studies utilizing the different Si/Al ratios. In such compounds, the structural network is mainly polysilicates with (–O–Si–O–Al–O–)*n* or (O–Si–O–Al–O–Si–O–Si–O–)*n*. Recently, geopolymers or inorganic polymers particularly of metakaolin-based geopolymer or metal oxide–carbon nanotubes as nanocomposite for the removal of MB have received researchers' attention [33]. Studies were also conducted using silicate geopolymer precursors characterized and tested for MB adsorption and exhibited adsorptive capacities of 2.84 to 3.01 mg/g [18], which are comparable to our finding of 3.28 mg/g. However, there is still a wide range of work that needs to be done to assess the sorption performance, adsorption influential factors, and adsorption mechanism of the Jordanian SGS [34,35]. Recently, some authors have evaluated the possible use of silica as a potential adsorbent material and whether it could be used for the removal of dyes [36].

In this work, Jordanian silica sand (silicates), the pure source of silica sand or glass sand SGS that is found naturally in vast amounts is used as an excellent nanomaterial adsorbent for MB dye. It is prepared and recommended for use as a low-cost, ease-of-synthesis method that can be carried out in a simple and cost-effective way in the laboratory without requiring expensive instruments [37]. The present study gives a convenient method, environment-friendly, and economical to use Jordanian SGS as an adsorbent to remove methylene blue MB dye from polluted water. The structural and morphological properties of the prepared SGS adsorbent were characterized by Fourier-transform infrared spectroscopy (FTIR), Brunauer–Emmett–Teller (BET), scanning electronic microscopy (SEM), and elemental analyses. The adsorption properties of the SGS were investigated by using the batch method under different conditions such as the effect of mass, pH with zeta potential, contact time, initial dye concentration, and temperature on the removal of MB from the aqueous solution. The adsorption kinetics, the isotherm of the adsorption, thermodynamics data, and reusability were investigated.

2. Experimental set-up

2.1. Materials and instruments

All chemicals used in this work were of analytical grade and used without any purification and were purchased from the Serono Jordan Company, a regional distributor of Sigma-Aldrich, Merck Company, Germany. Perchloric acid ($HClO_4$, 70%), hydrochloric acid, (HCl, 37%), nitric acid (HNO_3, 65%), hydrofluoric acid (HF, 48%), buffer solution pH (2,4,7,8,9,10,12), multi-element standard solution (Na, K, Fe, Al, and Ti) 1,000 ppm, and silica standard solution 1,000 ppm. Ultrasonic Bath, Elmasonic S150, Centrifuge Unit Seta, (UK) FTIR IRAffinity-1S, Shimadzu. The concentration of MB was quantitatively determined using the spectrophotometer JASCO V-630 UV/VIS. AAS atomic absorption spectrophotometer, Agilent Technologies Agilent 280FS AA, with hollow cathode lamp for (Al, Fe, Na, K, Si). Contour 800 F, Analytik Jena, Germany. Quantachrome, pore size analyzer by gas sorption. The scanning electron microscopic images we carried out at Petra University (Jordan), using EDX (JEOL JED-2300) SEM.

2.2. Preparation of glass sand sample

The composite sand sample was screened in Tyler screen sieves (325 μ) to reduce the size of silica sand and increase the surface area of the sand particle, then 100 g of the sample was transferred to a round bottom flask, with 500 mL of 10 M NaOH to reaction mixture then condensed at a temperature adjusted to 300°C for 3 h. Then, cooled at room temperature. The filtrate was separated from solid using filter paper (simple filtration) to remove unreacted sand particles,

then was transferred to a sonicator with an ice bath, pH electrode was added to monitor the filtrate pH, then a slowly and dropwise concentrated HCl was added until pH = 7. The solution mixture was sonicated for 30 min. A white slurry of silicic acid, $Si(OH)_4$ was formed. The reaction mixture was allowed to stand overnight at room temperature, to facilitate drying and polymerization.

2.3. Adsorption experiments

The adsorption experiments were carried out under different operating conditions of the adsorbent samples of silica sand composites with accurately weighted mass 0.20–1.5 g, contact time 0–60 min, initial solution pH 2–12, initial dye concentration 25–150 mg/L, and temperature 10°C–60°C. The mixture is thoroughly shaken in a capped container using a magnetic stirrer operating at 200 rpm for up to 30 min. Samples were then filtered, and the supernatant liquid was subjected to analysis. The concentration of residual MB dye was determined using a spectrophotometer at a wavelength of 664 nm. The removal efficiency was evaluated for MB adsorption capacities of SGS composite adsorbents. The optimum adsorption conditions were obtained by investigating the adsorption efficiency of different solution conditions including the effect of contact time, pH value, and initial concentration of MB dye (C_o). The efficiency of each adsorption process is expressed in terms of the removal percentage of MB from the solution and is defined as the ratio of the difference in the adsorbate concentration before and after adsorption ($C_o - C_e$), to the initial concentration of the MB dye in the aqueous solution (C_e) as shown in Eq. (1):

$$\%\text{Removal} = \frac{\left(C_o - C_e\right)}{C_o} \times 100 \tag{1}$$

The adsorption capacity at equilibrium q_e (mg/g) was determined using Eq. (2):

$$q_e = \frac{\left(C_i - C_e\right)V}{M} \tag{2}$$

where C_i (mg/L) is the initial concentration of MB dye solution, C_e (mg/L), is the liquid-phase equilibrium concentration of MB, m (g) is the weight of SGS, and V (L) is the volume of the MB solution.

2.4. Thermodynamic study of adsorption

Adsorption heat and enthalpy change are important thermodynamic variables with a strong temperature dependence that aid in the prediction of adsorption behavior [38]. The van't Hoff Eq. (3) [27], was used to analyze the values of K_L at various temperatures:

$$\ln K_L = -\frac{\Delta H^\circ}{RT} + \frac{\Delta S^\circ}{R} \tag{3}$$

where R is the universal gas constant (8.314 J/mol·K), and T is the absolute temperature; $K_L = q_e/C$ (in Kelvin) and ΔH° (J/mol) and ΔS° (J/mol·K) are the enthalpy and entropy changes, respectively. Plotting $\ln K_L$ vs. $1/T$ results in a straight line with slope and intercept of $-\Delta H^\circ/R$ and $\Delta S^\circ/R$, respectively. The Gibbs free energy of adsorption [ΔG° (J/mol)] was determined from Eq. (4):

$$\Delta G^\circ = \Delta H^\circ - T\Delta S^\circ \tag{4}$$

3. Results and discussion

Silica nanomaterials are used as nanoadsorbents because of their high porosity, non-toxic, high adsorption capacity, high surface area, excellent surface characteristics, low cost, and ease of regeneration. Table 1 shows the unique properties of SGS as an adsorbent.

3.1. Characterization of SGS adsorbent

The chemical composition of the Jordanian glass sand was found to be as follows: SiO_2 (97.93%), Na_2O (0.05%), K_2O (0.03%), CaO (0.52%), MgO (0.61%), Fe_2O_3 (0.09%), Al_2O_3 (0.65%), and moisture (0.08%). Quantitative elemental analysis of SGS and the above data reflect the high purity of Jordanian SGS as a source of silica.

3.2. FTIR spectral analysis

Fig. 1a shows the infrared spectra for the prepared SGS sample. The transmitted peaks at 458 and 578 cm^{-1} are caused by bending vibrations with asymmetric stretching vibrations for the siloxane group (Si–O–Si). The band at 850 cm^{-1} represents the bending wagging vibration for Si–O–Si, strong infrared bands can be observed. The Si–O–Si absorption becomes broader and more complex as the siloxane chains lengthen or branch, resulting in two or more overlapping bands. The band at 458 cm^{-1} and the band at 578 cm^{-1} are associated with the Si–O rocking in accordance with the literature [39]. The peak at 1,334 cm^{-1} is caused by (Si–O–Al) linkage with asymmetric stretching vibration, and the transmitted peaks at 1,640 cm^{-1} represent the bending scissoring vibration for adsorbed water. The peaks at 3,000–3,900 cm^{-1} caused by stretching vibration, confirm the presence of the Si–O–Si band, the Si–OH band, and the H–O–H band in silica [40]. Fig. 1b shows the SGS sample after adsorption of MB dye which confirms the presence of the dye with its distinct peaks at 3,425 cm^{-1} is O–H stretching vibration; these groups involve hydrogen bonds. The band observed at 2,700 and 3,032 cm^{-1} are assigned sp3 and sp2 C–H stretch, respectively. The bands observed at 1,354 and 1,492 cm^{-1}

Table 1
Surface and physical properties for silica glass sand

Solubility of silica glass sand in water	Soluble in water at pH < 3.00, and pH > 10.5
Pore volume, cc/g	0.058
Pore size width, nm	1.289
Surface area, m^2/g	50.954
pH points zero charge	pH_{pzc} = 6.7

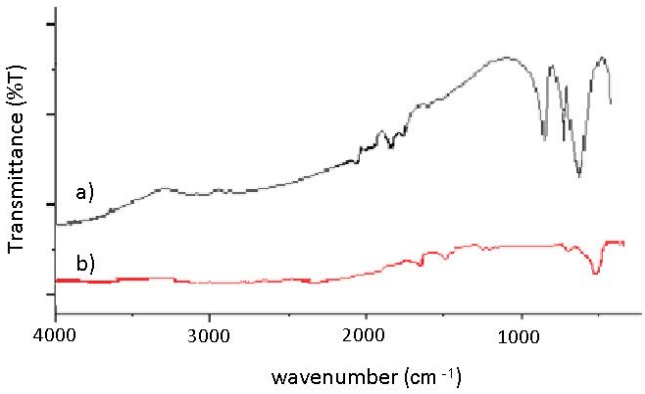

Fig. 1. Infrared spectrum of methylene blue dye (a) before and (b) after adsorption on silica glass sand.

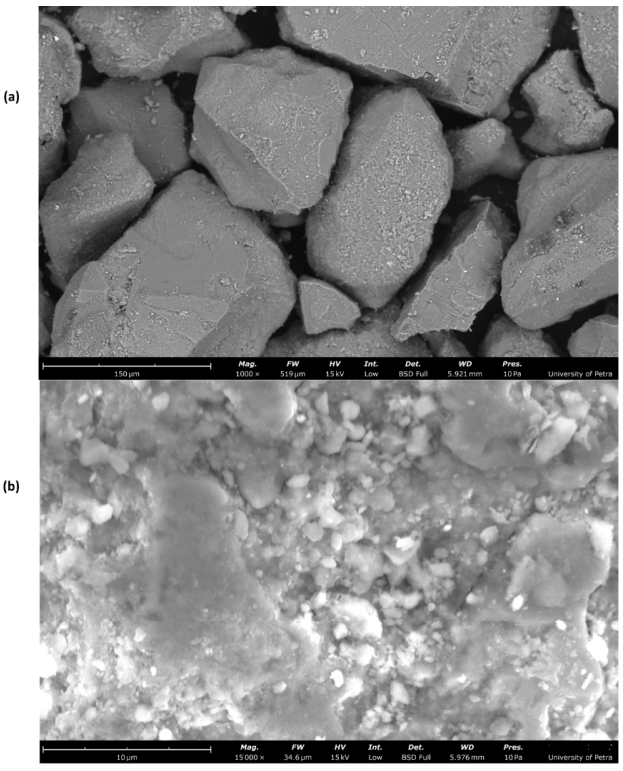

Fig. 2. Scanning electronic microscopy image of silica glass sand powder (a) before and (b) after adsorption of methylene blue.

are assigned to C–N and C=C stretching, respectively. The band at 1,600 cm^{-1} may present the C=C or C=N vibration in the aromatic ring. The peaks at 1,294 and 1,141 cm^{-1} are ascribed to C–C–H and C–O–H bending modes [41].

3.3. SEM for the prepared SGS nanoparticles

Fig. 2 shows SEM micrographs of the initial SGS prepared (Fig. 2a), and the SGS–MB (Fig. 2b), obtained after subsequent dye sorption. The SGS nanosheets are thoroughly covered with MB dye. SEM image of the SGS powder shows a porous matrix in which the sand maintains the sheet-like morphology having various sizes [42]. The micrograph also shows a fractured morphology that MB-encapsulated within the nanosheets that are well separated with increased thickness. The SGS powder exhibits a wide size distribution also determined in the next section of BET analysis. Flat cleavage-like surfaces are discernible in micron-sized particles [43]. The flat sheet shapes suggest that the silica glass particles are thick and platelike, rather than spherical or regularly shaped. This can be useful for understanding how the particles might pack together in a bulk material, which can improve properties like porosity, permeability, and mechanical strength for dye adsorption.

3.4. Pore size examination (BET analysis) for the prepared SGS nanoparticles

Nano silica particles are characterized by BET analysis for their porosity nature; this property is a characteristic that distinguishes SGS with a large surface area and efficient adsorption of the MB dye. In which, there is a tendency in the solid surface of silica to attract and adsorb MB molecules giving rise to an increase in the amount of dye adsorption and subsequently enhancing its removal efficiency. The obtained data from the pore size analysis of the SGS sample gave a pore volume = 0.058 cc/g, surface area = 50.954 m^2/g, and pore width = 1.289 nm, respectively.

3.5. Effect of operating parameters

3.5.1. Effect of adsorbent dosage

The dosage of adsorbent is an important parameter in the determination of the capacity of an adsorbent for a given initial concentration of the adsorbate at the operating conditions. The effect of SGS dose, varying from 0.2 to 1.5 g, for MB adsorption is depicted in Fig. 3a. It is apparent that the percent removal of MB increases with the increasing weight of SGS until 0.8 g. However, once all MB is adsorbed, additional adsorption sights from SGS will be insignificant. By increasing the dose, more surface area is available for adsorption due to an increase in active sites on the adsorbent then making it easier for more MB molecules to be moved to the sorption sites. These observations agree with other reports in the literature on the sorption of MB dye molecules by different sand or clay materials [44,45]. From the obtained results the optimal adsorbent dose selected for further studies is 0.8 g.

3.5.2. Effect of pH on removal efficiency and pH point of zero charge (pH_{pzc}) of SGS

The aqueous media pH governs the adsorption of dye molecules and affects the protonation of the active functional sites on the sorbent surface [46]. It has clearly been identified as the most important variable affecting adsorption onto solid-phase adsorbent, partly because small hydrogen ions compete with the protonated silica surface. To study the effect of pH on MB adsorption using SGS particles, adsorption experiments were conducted by varying the pH from 2 to 12. The results obtained are presented in Fig. 3b. With the increase of the initial pH, an increase in the

adsorption rate of MB was observed up to pH 6. After this pH, when the pH value varies from 6–8, we observe a low decrease in the rate of MB adsorption on the SGS until pH 8 (88%–86%), an optimal value of pH 6 was fixed. It follows from the theory of acid–base equilibria that, in the pH range 2–6, the binding of cationic MB molecules is determined primarily by the state of dissociation of the weak acidic groups. Carboxyl groups (–COOH) are the main groups to form hydrogen bonds with the polar silica surface of the adsorbent. At pH 6–8, there are fewer numbers of competing hydrogen ions and more surface negative charges

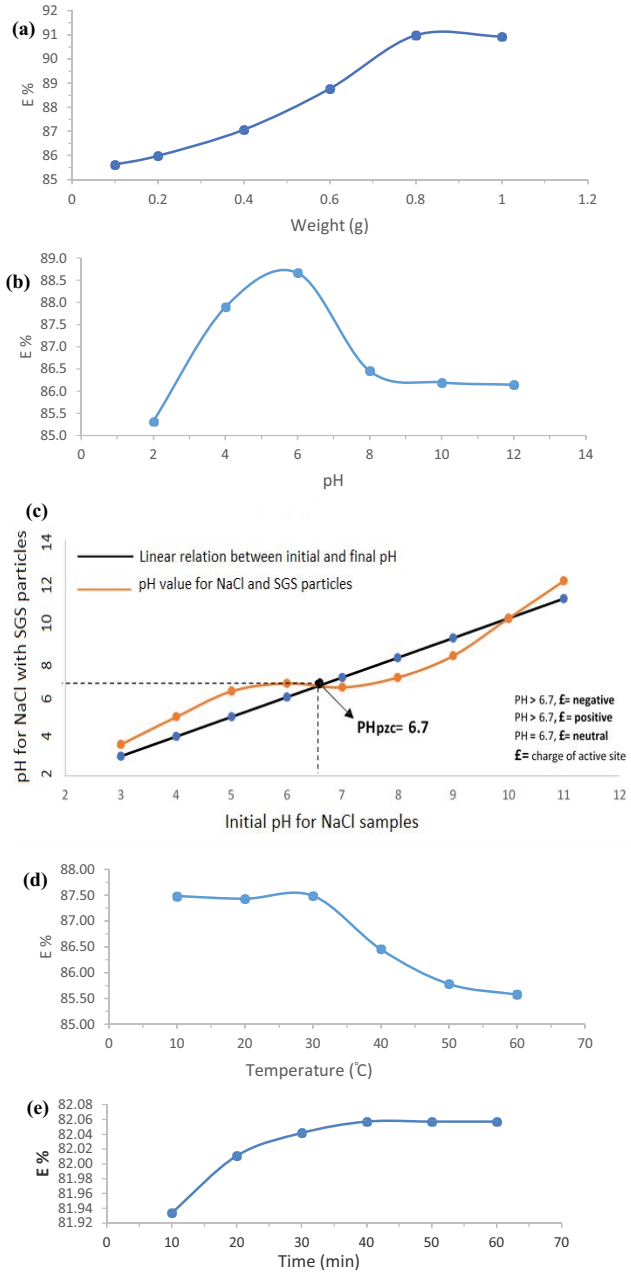

Fig. 3. (a) Effect of the adsorbent silica glass sand dosage, (b) effect of pH, (c) pH_{pzc} (point of zero charge) for silica glass sand, (d) effect of temperature, and (e) effect of contact time on the percent removal of methylene blue.

which are exposed to cationic MB resulting in greater MB sorption. But for pH greater than 8, a decrease in adsorption was observed for MB, this might be due to the lower polarity of MB at higher pH values [47]. At higher pH values, the lower number of H^+ with lesser negative surface charge results in less positive MB molecules adsorption. In order to confirm this result, the pH_{pzc} of the adsorbent is determined. The zero point of charge (PZC) is defined as the number of positive charges equal to the number of negative charges that exist on the surface of the adsorbent. The data obtained through the pH drift method experiment [48], for SGS and NaCl, was plotted, and the charge density on the active site of SNP_S (adsorbent) was characterized as shown in Fig. 3c. The pH_{pzc} of the SGS and the pH_{pzc} value of the adsorbent was found almost to be 6.7. Thus, at pH < 6.7, the surface of the SGS is positively charged and becomes negatively charged at pH > 6.7. Therefore, with increasing pH above pH_{pzc} = 6.7, the removal of cationic dye by the SGS increased slightly. The removal increase can be explained by electrostatic attraction between the particles of the SGS, which is negatively charged, and the cationic dye, which is positively charged [49]. These results show that the attraction between the silica framework (negatively charged) and the methylene blue (positively charged) depends on pH.

3.5.3. Effect of temperature

To investigate the effect of the temperature (10°C, 20°C, 30°C, 40°C, 50°C, and 60°C) on the MB dye adsorption, the experiments were conducted at a constant concentration of 2.0 ppm, constant mass of 0.2 g, pH = 6, and given time of 30 min. The results are given in Fig. 3c. As can be seen from the figure, the adsorption of MB onto the surface of SGS takes place quickly for three temperatures until 30°C. The absorbed amount of MB molecules sharply decreases when increasing the temperature from 30°C to 60°C. The observed drop in the adsorption capacity with an increase of temperature indicated that impenitent temperatures are in favor of MB molecules adsorption onto the SGS particles. This may be due to a tendency for the MB molecules to describe and move from the solid phase back to the aqueous phase when the temperature of the solution increases. This observation gives rise to suggest a mechanism of the physical adsorption process of MB molecules that involves an electrostatic interaction with the SGS surface for the adsorption [50]. This is also confirmed by the thermodynamic study given in Fig. 11 which means that the adsorption process has an exothermic nature. Similar behavior has been found by Sari and Tuzen [51].

3.5.4. Effect of contact time

The effect of contact time on the removal ability of MB was studied for 0.8 g mass of the adsorbent from 5 to 60 min. The initial MB dye concentration was fixed at 2.0 ppm, with interval shaking, at a temperature of 30°C, and solution pH at 6. Fig. 3d shows a rapid initial uptake rate of MB at the beginning until 30 min and, thereafter, the adsorption rate became almost constant. The initial increase in the extent of adsorption may be due to the fact that initially all sites on the surface of the adsorbent were vacant and the MB molecules

concentration was high. Consequently, the amount of MB species uptake decreases with the increase in contact time on the surface of SGS because of occupying vacant sights. Moreover, when adsorption involves a surface reaction process, it is more favorable that rapid initial adsorption would occur. Then, gradually lower adsorption would follow with time and the removal percentage would practically remain constant [52]. According to the results obtained at a given mass of 0.8 g, the equilibrium time found is 30 min.

3.5.5. Effect of the initial concentration of the MB dye

The effect of the initial MB concentration on the adsorption rate was investigated in the range of 25–125 ppm in a neutral to slightly acidic media (pH = 6–7). The results are presented in Fig. 4a for the effect of the concentration of MB on the adsorption capacity q_e. It can be seen in Fig. 4b that the percentage of removal increased with increasing initial MB concentration. The lower uptake at higher concentrations resulted from an increased ratio of the initial number of moles of MB molecules to the available sights and surface area in which fractional adsorption becomes independent of the initial concentration of the dye. For a given fixed adsorbent dose, the total number of available adsorption sites is limited thereby adsorbing more molecules became difficult after reaching the equilibrium point, thus resulting in a decrease or constant in the removal of MB molecules corresponding to the increase in the initial concentration. Related results were previously reported by other researchers [53].

3.6. Adsorption isotherms

The main goal of the adsorption isotherms was to establish the maximum amount of MB that a given mass of sand could adsorb. We employed several isotherm models to pinpoint the site of the MB's equilibrium between solution and sand mass. Two of the most common isotherms are the Langmuir monolayer adsorption model and the Freundlich multilayer adsorption model.

3.6.1. Langmuir isotherm

The foundation of the Langmuir model is the monolayer adsorption of solute particles into a finite number of identical places on the surface of the sorbent [54]. This hypothesis states that adsorbed molecules cannot move across surfaces or interact with one another. The linear form of the Langmuir model is as follows:

$$\frac{C_e}{q_e} = \frac{1}{bQ_o} + \frac{1}{Q_o}C_e \tag{5}$$

where C_e is the equilibrium MB concentration in solution (mg/L), b is the Langmuir affinity constant (L/mg), Q_o is the capacity for adsorption at equilibrium (mg/g), and q_e is the amount of MB adsorption per mass of adsorbent (sand), and it may be calculated using Eq. (2). A plot of (C_e/q_e) vs. (C_e) will provide a straight line with a slope of ($1/Q_o$) and an intercept of ($1/bQ_o$) if the Langmuir isotherm best fits the experimental data. The Langmuir parameters are determined using these plots (Fig. 5).

C_e/q_e vs. C_e (Fig. 5) was found to be linear with a negative slope, which shows that the examined system's adsorption behavior deviates from the fundamental assumption of the Langmuir technique. As a result, we performed additional analyses using various different adsorption models on the data. This gives strong proof that the adsorption of MB on

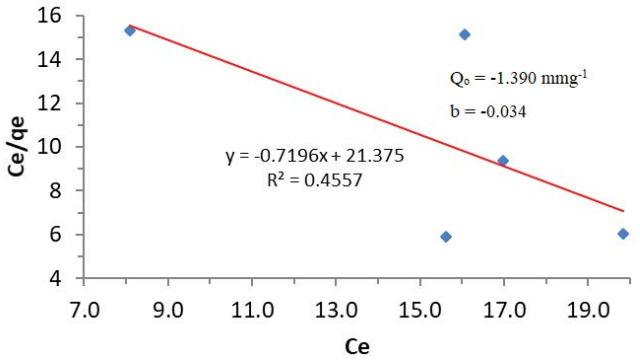

Fig. 5. Langmuir plots showing the adsorption of methylene blue on silica glass sand (at 30 min, pH 6, 20°C, V = 25 mL, m = 0.80 g, and C_o = 100 mg/L), and values for the isothermal constants and correlation coefficients (R^2).

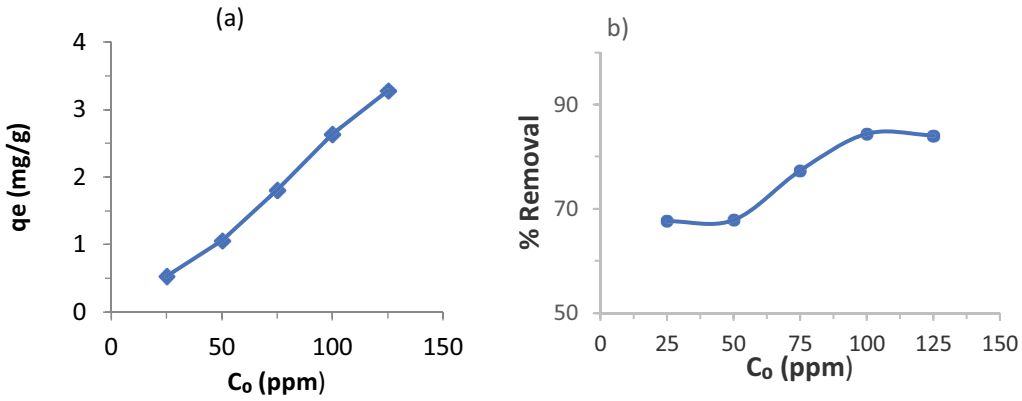

Fig. 4. (a) Amount of methylene blue adsorbed per mass of silica glass sand (mg/g) at various adsorbate concentrations and (b) methylene blue removal percentage at various methylene blue concentrations.

sand does not strictly adhere to a monolayer coverage and that chemisorption is not the main interaction between the MB adsorbate and the sand adsorbent.

3.6.2. Temkin isotherm

The Temkin isotherm model predicts that adsorbate/adsorbent interactions result in a linear decrease in the heat of adsorption for all adsorbate molecules with increasing adsorbent surface coverage. A regular distribution of binding energies up to a maximum binding energy, according to the model, is what defines adsorption. The linear form's expression is [55]:

$$q_e = \frac{RT}{b}\ln K_T + \frac{RT}{b}\ln C_e \quad (6)$$

where T stands for the absolute temperature (K), b for the heat of adsorption constant, K_T for the equilibrium binding constant corresponding to the maximum bending energy (L/mg), and R for the universal constant (8.314 J/K·mol).

Plotting (q_e) vs. ($\ln C_e$) results in a straight line with a slope of RT/b and an intercept of ($RT \ln K_T$)/b (Fig. 6). Based on the low correlation coefficient value R^2 of 0.6508, it is evident from the figure that the experimental data are not well suited to the Temkin isotherm.

3.6.3. Freundlich isotherm

On heterogeneous surfaces, the Freundlich isotherm model predicts that there would be a number of non-ideal adsorption layers. It suggests that stronger binding sites are exploited first, followed by weaker ones. In other words, when site occupation rises, the binding strength decreases. The linear form is seen in [56]:

$$\log q_e = \log K_F + \frac{1}{n}\log C_e \quad (7)$$

where the heterogeneity coefficient (n) defines how favorable an adsorption process is (g/L), and the Freundlich constant (K_F) relates to adsorption capacity (mg/g). Plotting ($\log q_e$) vs. ($\log C_e$) results in a straight line with slope (1/n) and intercept ($\log K_F$) (Fig. 7). The correlation coefficient value R^2 = 0.7606 indicates that the adsorption of MB on sand is predominantly physical multilayer adsorption that follows Freundlich equation, in contrast to the results from the Temkin isotherm model, as shown in the picture. The Temkin and Freundlich isotherms were used to fit the experimental data, and (Fig. 7) reports the parameters of the Freundlich isotherm for the adsorption of MB on the sand, as well as the correlation coefficient, values R^2.

3.7. Adsorption kinetics

The kinetics of adsorption were used to examine the process by which specific concentrations of MB diffuse from a solution to a boundary layer of the water surrounding the sand phase. The kinetics of MB adsorption onto sand was investigated by collecting solution samples and analyzing them at intervals of 10, 20, 30, 40, 50, and 60 min. At the optimal adsorption circumstances of 0.8 g of constant sand mass in a 25 mL solution at 20°C, pH 6, and 100 mg/L of constant beginning metal ion concentration, all kinetic tests were carried out. One can use Eq. (2) to calculate the amount of adsorption at time t. The kinetic data for the adsorption of MB onto sand were examined using Lagergren's pseudo-first-order, pseudo-second-order, and intraparticle diffusion models. The parameters of these models were calculated and summarized in Table 2.

3.7.1. Pseudo-first-order kinetics

The pseudo-first-order kinetics model [57] is the most widely used approach for explaining the kinetic process of liquid–solid phase adsorption or for the adsorption of adsorbate from an aqueous solution. The linear form of this model is as follows:

$$\log\left(q_e - q_t\right) = \log q_e - \frac{K_1}{2.303}t \quad (8)$$

where q_e is the mass (mg) of MB adsorbed per gram of sand at equilibrium; q_t is the mass (mg) of MB adsorbed per gram

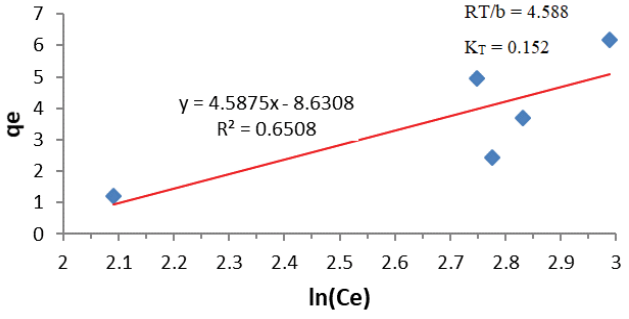

Fig. 6. Temkin plot shows the adsorption of methylene blue on silica glass sand (at 30 min, pH 6, 20°C, V = 25 mL, m = 0.80 g, and C_o = 100 mg/L), and values for the isothermal constants and correlation coefficients (R^2).

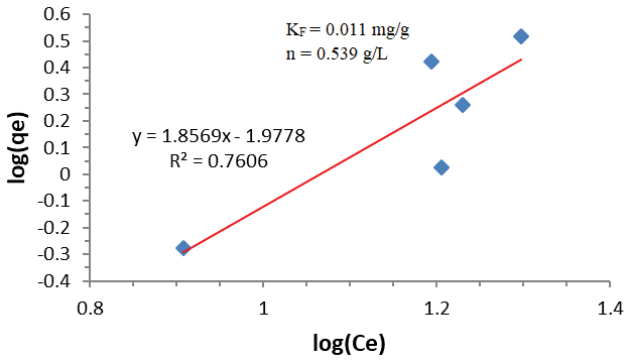

Fig. 7. Freundlich plots show the adsorption of methylene blue on silica glass sand (at 30 min, pH 6, 20°C, V = 25 mL, m = 0.80 g, and C_o = 100 mg/L), and values for the isothermal constants and correlation coefficients (R^2).

Table 2
Parameters for the methylene blue adsorption on silica glass sand using pseudo-first-order, pseudo-second-order, and intraparticle diffusion kinetic models

Adsorbate	Adsorption kinetics models					
	Pseudo-first-order		Pseudo-second-order		Intraparticle diffusion	
	q_e (mg/g)	K_1 (mg/g·min)	q_e (mg/g)	K_2 (g/mg·min)	C (mg/g)	K_P (mg/g·min$^{0.5}$)
Methylene blue	0.867	0.0002	2.565	18.759	2.557	0.0012

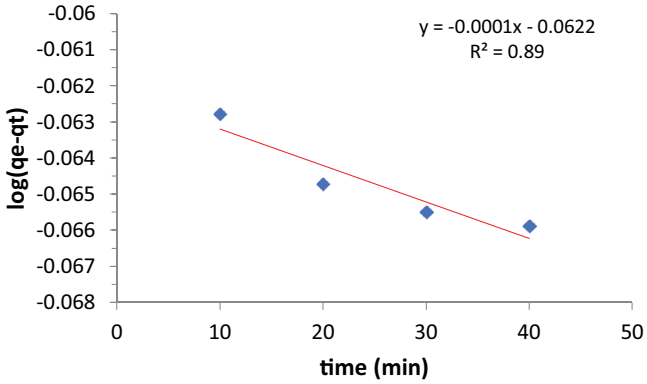

Fig. 8. Pseudo-first-order kinetic model showing the adsorption of methylene blue on silica glass sand (at 30 min, pH 8, 25°C, V = 25 mL, m = 0.50 g, and C_o = 100 mg/L).

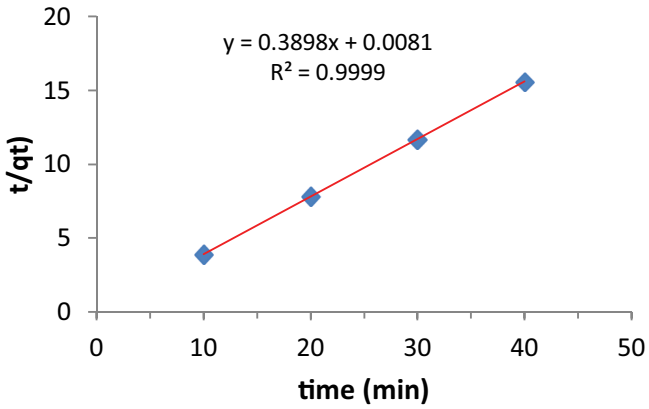

Fig. 9. Pseudo-second-order kinetic model showing the adsorption of methylene blue on silica glass sand (at 30 min, pH 8, 25°C, V = 25 mL, m = 0.50 g, and C_o = 100 mg/L).

of sand at time t; and K_1 is the rate constant for the pseudo-first-order adsorption model (mg/g·min). The log($q_e - q_t$) against the t graph can be used to compute K_1. For the hypothetical first-order adsorption, such a plot will produce a straight line with (logq_e) as the intercept and ($-K_1$/2.303) as the graph's slope (Fig. 8).

3.7.2. Pseudo-second-order kinetics

The adsorption kinetics can also be explained by a pseudo-second-order model. This equation results in the linear version of the model:

$$\frac{t}{q_t} = \frac{1}{K_2 q_e^2} + \frac{1}{q_e} t \tag{9}$$

The pseudo-second-order adsorption rate constant is denoted by K_2. If experimental data support this concept, plotting t/q_t vs. t yields a linear relationship, and from this relationship, K_2 and q_e may be computed from the slope and intercept of the graph (Fig. 9).

3.7.3. Intraparticle diffusion kinetic model

The formula for the intraparticle diffusion model is:

$$q_t = K_p t^{0.5} + C \tag{10}$$

where the constants K_P and C stand for the diffusion rate (mg/g·min$^{0.5}$) and the thickness of the boundary layer (mg/g), respectively. The intraparticle diffusion kinetic model's plot of q_t vs. $t^{0.5}$ demonstrates a linear relationship with constant C as the y-intercept and K_P as the slope (Fig. 10). The predicted values for the MB adsorptions on the sand composite were found to be consistent with the experimental findings (Table 2). The predicted q_e value (from second-order kinetics) for the adsorption of MB at 2.565 mg/g is equivalent to the actual result at 2.637 mg/g, in contrast to the calculated q_e value from first-order kinetics at 0.867 mg/g. Further evidence that the second-order kinetics mechanism was used in the adsorption of MB comes from the second-order kinetics correlation coefficient value, which is close to unity at 0.9999.

3.8. Thermodynamics analysis

Using Fig. 11, determine the values for $\Delta H°$, $\Delta S°$, and $\Delta G°$ presented in (Table 3). Because of the interaction between active sites and MB molecules, the negative values of $\Delta S°$ and $\Delta H°$, respectively revealed the high orderliness of the adsorption system at equilibrium and pointed out the exothermic nature of the adsorption process. According to the negative value of $\Delta G°$, the adsorption process is spontaneous. It was implied that adsorption was less favorable at higher temperatures by the fact that negative values of $\Delta G°$ reduced as temperature increased [58].

3.9. Desorption and reusability of SGS

A desorption study is one of the significant characteristics to show the reusability of adsorbent several times and

Table 3
Thermodynamic parameters of SGS-based methylene blue adsorption

Temp.	1/T	C_e	q_e	k_e	lnk_e	$\Delta G°$	$\Delta H°$	$\Delta S°$
K	K^{-1}		mg/g	L/g		(kJ/mol)	(kJ/mol)	(J/mol·K)
283	0.0035	2.529	3.046	1.205	0.1862	–0.438		
293	0.0034	2.601	3.044	1.170	0.1573	–0.383		
303	0.0033	2.698	3.041	1.127	0.1194	–0.301	–3.195	–8.613
313	0.0032	2.796	3.038	1.086	0.0828	–0.216		
323	0.0031	2.915	3.034	1.041	0.0401	–0.108		
333	0.0030	3.018	3.031	1.004	0.0044	–0.012		

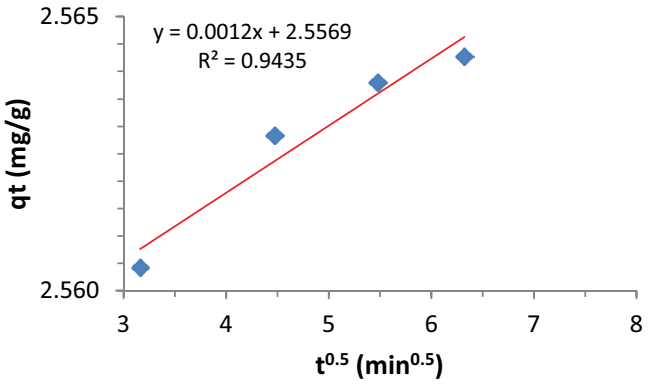

Fig. 10. Intraparticle diffusion kinetic model showing the adsorption of methylene blue on silica glass sand (at 30 min, pH 8, 25°C, V = 25 mL, m = 0.50 g, and C_o = 100 mg/L).

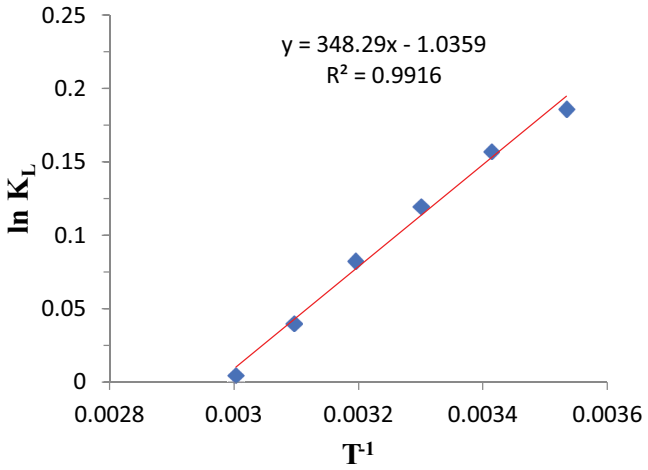

Fig. 11. Plot of lnK_L against 1/T for the adsorption of methylene blue onto silica glass sand.

determine its advantages such as stability and recovery in reducing cost [59]. Using 0.5 g after saturation with 100 ppm MB dye, the desorption has been achieved by using 100 mL of 0.01 M HCl solution at the optimized parameters of pH and temperature to recover 88.40% of the dye, in the first use cycle as shown in Fig. 12. The graph also indicates that the desorption process was repeated four times in order to

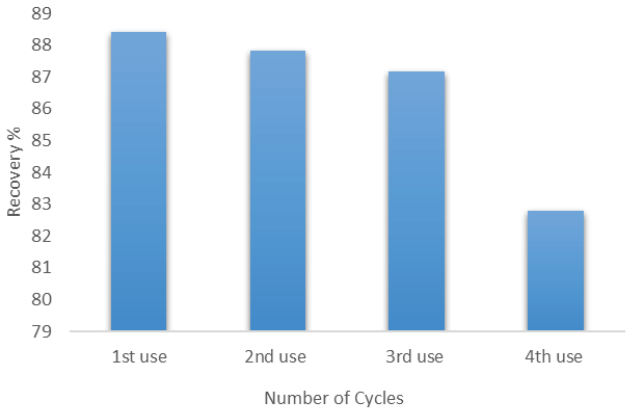

Fig. 12. Regeneration and reusability study of the silica glass sand material to remove methylene blue dye.

examine the efficiency of the material with recovery 87.83%, 87.16%, and 82.79% for second, third, and fourth use, respectively. The slight decrease in the removal efficiency of SGS is due to the gradual saturation of the available places in the adsorbents [60]. After the fourth cycle, a reduction of the percentage adsorption was only 5.81%. This observation implies that SGS can be considered an effective and recyclable material for the adsorptive removal of MB dye.

4. Conclusions

In this work, natural silica SiO_2 nanoparticle was successfully prepared from natural Jordanian glass sand by means of sol–gel and hydrothermal methods. The silica powder of (SGS) was successfully characterized and tested as an effective low-cost adsorbent in the removal of MB dye from water. The kinetic, thermodynamic, and isothermal behavior of MB dye adsorption onto SGS is the subject of the current work. It was shown that the kinetics data of MB dye adsorption on SGS matched the pseudo-second-order kinetic model with a correlation coefficient (R^2 > 0.99) that is as high as absolute linearity (R^2 = 1.00). 100 ppm of MB, pH 6, 20°C, 0.8 g of sand, 25 mL of solution, and 30 min of contact time were the ideal adsorption conditions. The outcomes were examined using the adsorption isotherm Langmuir, Freundlich, and Temkin models. The adsorption parameters for the three isotherm models were determined. The results were well described by Freundlich isotherm

models. The adsorption is physisorption, as indicated by the low heat of adsorption ($\Delta H°$ = –3.20 kJ/mol). The adsorption process was exothermic and spontaneous, as shown by the thermodynamic parameters $\Delta G°$, $\Delta H°$, and $\Delta S°$. The fact that the values of the $\Delta G°$ decrease with rising temperature suggests that the spontaneous impact is becoming more pronounced. The SGS adsorbent is a potential low-cost material for the effective and economical removal of MB from an aqueous solution with excellent recyclability.

References

[1] D. Mohan, A. Sarswat, Y.S. Ok, C.U. Pittman Jr., Organic and inorganic contaminants removal from water with biochar, a renewable, low cost and sustainable adsorbent: a critical review, Bioresour. Technol., 160 (2014) 191–202.

[2] R. Srinivasan, Advances in the application of natural clay and its composites in the removal of biological, organic, and inorganic contaminants from drinking water, Adv. Mater. Sci. Eng., 2011 (2011) 1–17.

[3] B. Senthil Rathi, P. Senthil Kumar, Application of adsorption process for effective removal of emerging contaminants from water and wastewater, Environ. Pollut., 280 (2021) 116995, doi: 10.1016/j.envpol.2021.116995.

[4] R. Saxena, M. Saxena, A. Lochab, Recent progress in nanomaterials for adsorptive removal of organic contaminants from wastewater, ChemistrySelect, 1 (2020) 335–353.

[5] R.M.A.Q. Jamhour, T.S. Ababneh, A.I. Al-Rawashdeh, G.M. Al-Mazaideh, T. M.A. Al Shboul, T.M.A. Jazzazi, Adsorption isotherms and kinetics of Ni(II) and Pb(II) ions on new layered double hydroxides-nitrilotriacetate composite in aqueous media, Adv. Anal. Chem., 6 (2016) 17–33.

[6] C. Arora, D. Bharti, S. Soni, A. Patel, R. Singh, Chapter 20 – Adsorptive Removal of Hazardous Dyes From Industrial Waste Using Activated Carbon: An Appraisal, P. Singh, P. Verma, R. Singh, A. Ahamad, A.C.S. Batalhão, Eds., Waste Management and Resource Recycling in the Developing World, Elsevier, 2023, pp. 455–483.

[7] M. Sardar, M. Manna, M. Maharana, S. Sen, Remediation of Dyes from Industrial Wastewater Using Low-Cost Adsorbents, Inamuddin, M. Ahamed, E. Lichtfouse, A. Asiri, Eds., Green Adsorbents to Remove Metals, Dyes and Boron from Polluted Water, Environmental Chemistry for a Sustainable World, Vol. 49, Springer, Cham, 2021. https://doi.org/10.1007/978-3-030-47400-3_15

[8] P.N. Karungamye, Methods used for removal of pharmaceuticals from wastewater: a review, Appl. J. Environ. Eng. Sci., 6 (2020) 6–4.

[9] K.G. Pavithra, V.J.J.O.I. Jaikumar, Removal of colorants from wastewater: a review on sources and treatment strategies, J. Ind. Eng. Chem., 75 (2019) 1–19.

[10] H. Ghazal, E. Koumaki, J. Hoslett, S. Malamis, E. Katsou, D. Barcelo, H. Jouhara, Insights into current physical, chemical and hybrid technologies used for the treatment of wastewater contaminated with pharmaceuticals, J. Cleaner Prod., 361 (2022) 132079, doi: 10.1016/j.jclepro.2022.132079.

[11] K.-T. Chung, Azo dyes and human health: a review, J. Environ. Sci. Health., Part C Environ. Carcinog. Ecotoxicol. Rev., 34 (2016) 233–261.

[12] M. Rafatullah, O. Sulaiman, R. Hashim, A. Ahmad, Adsorption of methylene blue on low-cost adsorbents: a review, J. Hazard. Mater., 177 (2010) 70–80.

[13] A.K.D. Alsukaibi, Various approaches for the detoxification of toxic dyes in wastewater, Processes, 10 (2022) 1968, doi: 10.3390/pr10101968.

[14] M.R. Islam, M.G. Mostafa, Textile dyeing effluents and environment concerns: a review, J. Environ. Sci. Nat. Resour., 11 (2018) 131–144.

[15] Y. Zhou, J. Lu, Y. Zhou, Y. Liu, Recent advances for dyes removal using novel adsorbents: a review, Environ. Pollut., 252 (2019) 352–365.

[16] J. Jeevanandam, A. Barhoum, Y.S. Chan, A. Dufresne, M.K. Danquah, Review on nanoparticles and nanostructured materials: history, sources, toxicity and regulations, Beilstein J. Nanotechnol., 9 (2018) 1050–1074.

[17] H. Sies, D.P. Jones, Reactive oxygen species (ROS) as pleiotropic physiological signalling agents, Nat. Rev. Mol. Cell Biol., 21 (2020) 363–383.

[18] A. Giwa, A. Yusuf, H.A. Balogun, N.S. Sambudi, M.R. Bilad, I. Adeyemi, S. Chakraborty, S. Curcio, Recent advances in advanced oxidation processes for removal of contaminants from water: a comprehensive review, Process Saf. Environ. Prot., 146 (2021) 220–256.

[19] A. Rafiq, M. Ikram, S. Ali, F. Niaz, M. Khan, Q. Khan, M. Maqbool, Photocatalytic degradation of dyes using semiconductor photocatalysts to clean industrial water pollution, J. Ind. Eng. Chem., 97 (2021) 111–128.

[20] E. Oyarce, K. Roa, A. Boulett, S. Sotelo, P. Cantero-López, J. Sánchez, B.L. Rivas, Removal of dyes by polymer-enhanced ultrafiltration: an overview, Polymers, 13 (2021) 3450, doi: 10.3390/polym13193450.

[21] M.R. Samarghandi, A. Dargahi, A. Shabanloo, H.Z. Nasab, Y. Vaziri, A. Ansari, Electrochemical degradation of methylene blue dye using a graphite doped PbO_2 anode: optimization of operational parameters, degradation pathway and improving the biodegradability of textile wastewater, Arabian J. Chem., 13 (2020) 6847–6864.

[22] W. Xiao, X. Jiang, X. Liu, W. Zhou, Z.N. Garba, I. Lawan, Z. Yuan, Adsorption of organic dyes from wastewater by metal-doped porous carbon materials, J. Cleaner Prod., 284 (2021) 124773, doi: 10.1016/j.jclepro.2020.124773.

[23] A. Mariyam, J. Mittal, F. Sakina, R.T. Baker, A.K. Sharma, A. Mittal, Efficient batch and fixed-bed sequestration of a basic dye using a novel variant of ordered mesoporous carbon as adsorbent, Arabian J. Chem., 14 (2021) 103186, doi: 10.1016/j.arabjc.2021.103186.

[24] W.A. Shaikh, A. Kumar, S. Chakraborty, Mu. Naushad, R.U. Islam, T. Bhattacharya, S. Datta, Removal of toxic dye from dye-laden wastewater using a new nanocomposite material: isotherm, kinetics and adsorption mechanism, Chemosphere, 308 (2022) 136413, doi: 10.1016/j.chemosphere.2022.136413.

[25] R.M.A.Q. Jamhour, G.M. Al-Mazaideh, Treatment of chromium(III) in tannery wastewater using LDH incorporated with EDTA, J. Environ. Earth Sci., 4 (2014) 98–104.

[26] R. Foroutan, S.J. Peighambardoust, S. Hemmati, H. Khatooni, B. Ramavandi, Preparation of clinoptilolite/starch/$CoFe_2O_4$ magnetic nanocomposite powder and its elimination properties for cationic dyes from water and wastewater, Int. J. Biol. Macromol., 189 (2021) 432–442.

[27] D.M. EL-Mekkawi, F.A. Ibrahim, M.M. Selim, Removal of methylene blue from water using zeolites prepared from Egyptian kaolins collected from different sources, J. Environ. Chem. Eng., 4 (2016) 1417–1422.

[28] N. Danial, S.A. Mousavi, Dye removal from water and wastewater by nanosized metal oxides-modified activated carbon: a review on recent research, J. Environ. Health Sci. Eng., 18 (2020) 1671–1689.

[29] X. Fu, X. Chen, J. Wang, J. Liu, Fabrication of carboxylic function-alized superparamagnetic mesoporous silica microspheres and their application for removal basic dye pollutants from water, Microporous Mesoporous Mater., 139 (2011) 8–15.

[30] S. Sohni, R. Hashim, H. Nidaullah, J. Lamaming, O. Sulaiman, Chitosan/nano-lignin based composite as a new sorbent for enhanced removal of dye pollution from aqueous solutions, Int. J. Biol. Macromol., 132 (2019) 1304–1317.

[31] S.A. Jadhav, H.B. Garud, A.H. Patil, G.D. Patil, C.R. Patil, T.D. Dongale, P.S. Patil, Recent advancements in silica nanoparticles-based technologies for removal of dyes from water, Colloid Interface Sci. Commun., 30 (2019) 100181, doi: 10.1016/j.colcom.2019.100181.

[32] J. Chang, J. Ma, Q. Ma, D. Zhang, N. Qiao, M. Hu, H. Ma, Adsorption of methylene blue onto Fe_3O_4/activated montmorillonite nanocomposite, Appl. Clay Sci., 119 (2016) 132–140.

[33] V. Kumar, P. Saharan, A. Sharma, A. Umar, I. Kaushal, A. Mittal, Y. Al-Hadeethi, B. Rashad, Silver doped manganese oxide-carbon nanotube nanocomposite for enhanced dye-sequestration: isotherm studies and RSM modelling approach, Ceram. Int., 46 (2020) 10309–10319.
[34] V.O. Shikuku, S. Tome, D.T. Hermann, G.A. Tompsett, M.T. Timko, Rapid adsorption of cationic methylene blue dye onto volcanic ash-metakaolin based geopolymers, Silicon, 14 (2022) 9349–9359.
[35] B. Aouan, S. Alehyen, M. Fadil, M. El Alouani, H. Saufi, F. El Makhoukhi, M. Taibi, Development and optimization of geopolymer adsorbent for water treatment: application of mixture design approach, J. Environ. Manage., 338 (2023) 117853, doi: 10.1016/j.jenvman.2023.117853.
[36] S.A. Jadhav, H.B. Garud, A.H. Patil, G.D. Patil, C.R. Patil, T.D. Dongale, P.S. Patil, Recent advancements in silica nanoparticles-based technologies for removal of dyes from water, Colloid Interface Sci. Commun., 30 (2019) 100181, doi: 10.1016/j.colcom.2019.100181.
[37] S. Soni, P.K. Bajpai, D. Bharti, J. Mittal, C. Arora, Removal of crystal violet from aqueous solution using iron-based metal-organic framework, Desal. Water Treat., 205 (2020) 386–399.
[38] D. Das, N. Das, L. Mathew, Kinetics, equilibrium and thermodynamic studies on biosorption of Ag(I) from aqueous solution by macrofungus *Pleurotus platypus*, J. Hazard. Mater., 184 (2010) 765–774.
[39] K.A. Mauritz, R.M. Warren, Microstructural evolution of a silicon oxide phase in a perfluorosulfonic acid ionomer by an in-situ sol-gel reaction. 1. Infrared spectroscopic studies, Macromolecules, 22 (1989) 1730–1734.
[40] T. Uchino, T. Sakka, M. Iwasaki, Interpretation of hydrated states of sodium silicate glasses by infrared and Raman analysis, J. Am. Ceram. Soc., 74 (1991) 306–313.
[41] T.A. Saleh, S.H. Al-Ruwayshid, A. Sarı, M. Tuzen, Synthesis of silica nanoparticles grafted with copolymer of acrylic acrylamide for ultra-removal of methylene blue from aquatic solutions, Eur. Polym. J., 130 (2020) 109698, doi: 10.1016/j.eurpolymj.2020.109698.
[42] A. Darghouth, S. Aouida, B. Bessais, High purity porous silicon powder synthesis by magnesiothermic reduction of Tunisian silica sand, Silicon, 13 (2021) 667–676.
[43] L. Sheng, Y. Zhang, F. Tang, S. Liu, Mesoporous/microporous silica materials: preparation from natural sands and highly efficient fixed-bed adsorption of methylene blue in wastewater, Microporous Mesoporous Mater., 257 (2018) 9–18.
[44] P. Li, B. Gao, A. Li, H. Yang, Evaluation of the selective adsorption of silica-sand/unionized-starch composite for removal of dyes and cupper(II) from their aqueous mixtures, Int. J. Biol. Macromol., 149 (2020) 1285–1293.
[45] O.S. Bello, I.A. Bello, K.A. Adegoke, Adsorption of dyes using different types of sand, S. Afr. J. Chem., 66 (2013) 117–129.
[46] R. Lakshmipathy, N.C. Sarada, Adsorptive removal of basic cationic dyes from aqueous solution by chemically protonated watermelon (*Citrullus lanatus*) rind biomass, Desal. Water Treat., 52 (2014) 6175–6184.
[47] S.K. Panda, I. Aggarwal, H. Kumar, L. Prasad, A. Kumar, A. Sharma, N. Dai-Viet Vo, D.V. Thuan, V. Mishra, Magnetite nanoparticles as sorbents for dye removal, Environ. Chem. Lett., 19 (2021) 2487–2525.
[48] B. Silva, T. Tavares, Effect of pH on the removal of fluoxetine from aqueous solutions by granular activated carbon, Proceedings of the 4th International Conference, Porto, Portugal, Sep 25–26, 2017, pp. 69–71.
[49] M.E.L. Alouani, S. Alehyen, M.E.L. Achouri, M. Taibi, Removal of cationic dye-methylene blue-from aqueous solution by adsorption on fly ash-based geopolymer, J. Mater. Environ. Sci., 9 (2018) 32–46.
[50] F. Ferrero, Adsorption of methylene blue on magnesium silicate: kinetics, equilibria and comparison with other adsorbents, J. Environ. Sci., 22 (2010) 467–473.
[51] A. Sari, M. Tuzen, Cd(II) adsorption from aqueous solution by raw and modified kaolinite, Appl. Clay Sci., 88 (2014) 63–72.
[52] N. Kannan, M.M. Sundaram, Kinetics and mechanism of removal of methylene blue by adsorption on various carbons—a comparative study, Dyes Pigm., 51 (2001) 25–40.
[53] M. Doğan, H. Abak, M. Alkan, Adsorption of methylene blue onto hazelnut shell: kinetics, mechanism, and activation parameters, J. Hazard. Mater., 164 (2009) 172–181.
[54] I. Langmuir, The constitution and fundamental properties of solids and liquids. Part I. Solids, J. Am. Chem. Soc., 38 (1916) 2221–2295.
[55] S.H. Abbas, I.M. Ismail, T.M. Mostafa, A.H. Sulaymon, Biosorption of heavy metals, J. Chem. Sci. Technol., 3 (2014) 74–102.
[56] H. Freundlich, About Adsorption in Solutions: Habilitation Thesis by Which... to Hold Test Lecture "Capillary Chemistry and Physiology" Invites Dr. Herbert Freundlich, W. Engelman, 1906.
[57] S.K. Lagergren, About the theory of so-called adsorption of soluble substances, Sven. Vetenskapsakad. Handingarl., 24 (1898) 1–39.
[58] B. Meroufel, O. Benali, M. Benyahia, Y. Benmoussa, M.A. Zenasni. Adsorptive removal of anionic dye from aqueous solutions by Algerian kaolin: characteristics, isotherm, kinetic and thermodynamic studies, J. Mater. Environ. Sci., 4 (2013) 482–491.
[59] A.V. Baskar, N. Bolan, S.A. Hoang, P. Sooriyakumar, M. Kumar, L. Singh, K.H. Siddique, Recovery, regeneration and sustainable management of spent adsorbents from wastewater treatment streams, Sci. Total Environ., 822 (2022) 153555, doi: 10.1016/j.scitotenv.2022.153555.
[60] M.O. Omorogie, J.O. Babalola, E.I. Unuabonah, Regeneration strategies for spent solid matrices used in adsorption of organic pollutants from surface water: a critical review, Desal. Water Treat., 57 (2016) 518–544.